

# Influence of Co:Mn ratio on multiferroicity of $\text{Ca}_3\text{Co}_{2-x}\text{Mn}_x\text{O}_6$ around $x \sim 1$

P. Ding,<sup>1,2</sup> L. Li,<sup>2</sup> Y. J. Guo,<sup>2</sup> Q. Y. He,<sup>1</sup> X. S. Gao,<sup>1</sup> and J.-M. Liu<sup>1,2,3,a)</sup>

<sup>1</sup>Laboratory of Quantum Information Technology, School of Physics, South China Normal University, Guangzhou 510006, China

<sup>2</sup>Laboratory of Solid State Microstructures, Nanjing University, Nanjing 210093, China

<sup>3</sup>International Center for Materials Physics, Chinese Academy of Sciences, Shenyang 110016, China

(Received 29 April 2010; accepted 24 June 2010; published online 19 July 2010)

A series of polycrystalline  $\text{Ca}_3\text{Co}_{2-x}\text{Mn}_x\text{O}_6$  with  $0.93 < x < 1.07$  are prepared in order to investigate the effect of Co:Mn ratio around  $x \sim 1.0$  on the multiferroicity. It is found that the ferroelectric polarization  $P$  at low temperature shows significant dependence on the Co:Mn ratio, forming a V-shaped pattern with the lowest point at  $x \sim 0.99$ . It is proposed that the suppression of  $P$  with the Co:Mn ratio approaching to the best Co/Mn order originates from the disruption of the long range spin order. © 2010 American Institute of Physics. [doi:10.1063/1.3464289]

Multiferroics have drawn more and more attention due to their magnetoelectric coupling between ferroelectric (FE) and spin orders.<sup>1,2</sup> Among these multiferroics, the Ising chain magnet  $\text{Ca}_3\text{Co}_{2-x}\text{Mn}_x\text{O}_6$  ( $x \sim 1$ , abbreviated as CCMO hereafter) represents one of the frequently visited systems due to its fascinating multiferroicity,<sup>3–11</sup> whose structural origin and delicate nature of competition between the involved multi-fold interactions are addressed. CCMO consists of anisotropic spin chains, where  $\text{Co}^{2+}$  and  $\text{Mn}^{4+}$  ions align alternatively along the  $c$ -axis and form the  $\uparrow\uparrow\downarrow\downarrow$  spin order at low temperature ( $T$ ), with the  $\text{Co}^{2+}$  and  $\text{Mn}^{4+}$  spins  $S=1/2$  and  $S=3/2$ , respectively.<sup>3–6</sup> Separated by  $\text{Ca}^{2+}$  ions, each chain is surrounded by six equally spaced chains and forms a triangular arrangement on the  $a$ - $b$  plane. It is believed that for each chain, the bonds between the parallel spins are shortened while those connecting antiparallel ones are stretched because of the exchange striction ion associated with the symmetric superexchange, resulting in the electric dipoles defined along this specific chain.

In fact, there are two types of energetically degenerate spin chains, shown in Fig. 1(a), both of which require a well defined Co/Mn ionic order, leading to FE polarization  $P$  with opposite directions.<sup>3–5,7</sup> It seems that both the  $\uparrow\uparrow\downarrow\downarrow$  spin order and Co/Mn ionic order are the pre-requisites of the multiferroicity in CCMO. According to the axial next-nearest-neighbor Ising (model) model,<sup>3,4</sup> the competition between the nearest-neighbor (NN) and next-nearest-neighbor (NNN) intrachain interactions are responsible for the  $\uparrow\uparrow\downarrow\downarrow$  spin order, while such order in long-range is formed by the assistance of interchain interactions. Unfortunately, for CCMO, the interchain interactions on the  $a$ - $b$  plane are rather weak. As a result, the FE domains associated with the spin long-range order (LRO) are sensitive against thermal fluctuations and the measured  $P$  decreases rapidly with increasing  $T$ .<sup>3</sup> This explains the essential role that the intrachain LRO plays in generating the ferroelectricity at finite  $T$ .

The stoichiometric  $x=1$  sample exhibits a strict ionic order with Co/Mn ions occupying the trigonal and octahedral sites without fault, respectively.<sup>4</sup> While theoretical works mainly deal with CCMO exactly at  $x=1$ ,<sup>7–10</sup> it is surprising

to find that the spin LRO is available over a broad range of  $0.75 < x < 1.0$  but lost in the narrow vicinity of  $x=1.0$ . One reason for this “order-by-static-disorder” effect may be related to the ionic disorder around  $x \sim 1.0$  which would disrupt the long-range effective interactions.<sup>4</sup> Given this fact, one is allowed to argue that the delicate fluctuations of the Co:Mn ratio around  $x \equiv 1.0$  would make great impact on the spin LRO and thus the FE behavior. This is the major motivation of our work. Herein, we present careful experiments on the FE and magnetic behaviors of CCMO with the Co:Mn ratio slightly deviating from 1.0 from both sides.

A series of polycrystalline CCMO ( $0.93 < x < 1.07$ ) samples were prepared using the codeposition method. Powders of  $\text{Ca}(\text{NO}_3)_2 \cdot 4\text{H}_2\text{O}$ ,  $\text{Co}(\text{NO}_3)_2 \cdot 6\text{H}_2\text{O}$ , and  $\text{MnCl}_2 \cdot 4\text{H}_2\text{O}$  were dissolved in de-ionized (DI) water and  $\text{K}_2\text{CO}_3$  was used to deposit Ca, Co, and Mn ions. The depo-

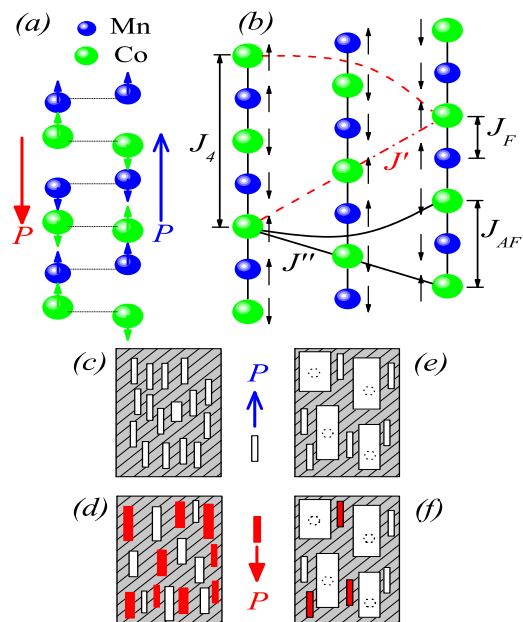


FIG. 1. (Color online) (a) Two configurations of the Ising chain in CCMO. The dashed line represents the original positions. (b) Interactions among spins in three NN chains, which forms an equilateral triangle on the  $a$ - $b$  plane. Schematic pictures of FE domains for sample at  $T \sim 2$  K are shown in (c)  $x=1$ , with electric field, (d)  $x=1$ , without electric field, (e)  $x \neq 1$ , with electric field, and (f)  $x \neq 1$ , without electric field.

<sup>a)</sup>Author to whom correspondence should be addressed. Electronic mail: liujm@nju.edu.cn.

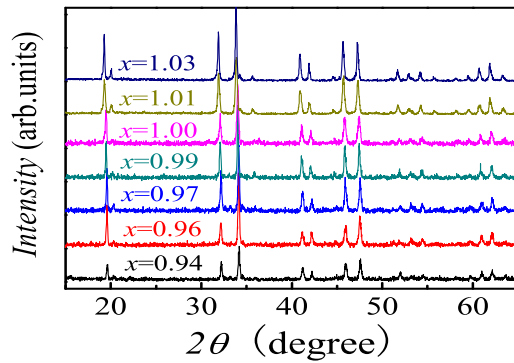


FIG. 2. (Color online) XRD spectra for CCMO with different  $x$ .

sition was then washed using DI water to remove KCl and  $\text{KNO}_3$ . After drying at  $80^\circ\text{C}$  for 12 h, the precipitation was calcined at  $700^\circ\text{C}$  for 24 h, pressed into pellets and then calcined at  $900^\circ\text{C}$  for 24 h. Here, it is addressed that many series of samples were prepared with the same procedure, accompanied with careful chemical composition analysis by means of electron microprobes and x-ray fluorescence spectroscopy. The measured Co:Mn ratios are consistent with the nominal values within the measuring uncertainties (parts per million level).

The sample crystallinity was characterized by x-ray diffraction (XRD) at room temperature, as shown in Fig. 2. All the samples are in single phase and the reflections are in good agreement with earlier reports on CCMO.<sup>11,12</sup>

Polarization  $P$  as a function of  $T$  was measured using the pyroelectric current method plus careful exclusion of other possible contributions.<sup>13</sup> The samples were first poled in a static electric field  $E=10$  kV/cm from 200 to 2 K and then the pyroelectric currents measured through warming the samples at rates of 2 to 6 K/min were integrated. Details of such measurements were reported in earlier work.<sup>11,12</sup> The dielectric constant ( $\epsilon$ ) was measured using HP4294 impedance analyzer at various frequencies (typically at  $f=100$  kHz). The dc magnetic susceptibility ( $\chi$ ) in response to  $T$  was measured using Quantum Design superconducting quantum interference device (SQUID).

We pay specific attention to the  $P(T)$  and  $P(H)$  data for all the samples. Figure 3(a) shows the  $P(T)$  data for  $x=0.96$ , 0.99, and 1.01. All these  $P$ - $T$  curves show similar features, i.e., rapid drop of  $P$  with  $T$  and almost disappearance of  $P$  at  $T>10$  K, consistent with earlier reports.<sup>3,5,11</sup> Nevertheless, it is indeed confirmed that the  $P$ - $T$  relation shows significant dependence on  $x$ . The measured  $P$  for  $x=0.96$  and  $x=1.01$  does not decay down to zero until a higher  $T$  than that for  $x=0.99$ , indicating that the robustness of the FE order is  $x$ -dependent. For a clearer presentation, one plots the measured  $P$  at  $T=2$  K as a function of  $x$ , as shown in the inset of Fig. 3(a), where a clear V-shaped pattern is observed. The valley appears at  $x\sim 0.99$ , indeed close to the strict Co/Mn ionic order point  $x=1.0$ . Deviating from this point leads to a significant enhancement of  $P$ . The present data do demonstrate the remarkable impact of the Co:Mn ratio on the ferroelectricity. In addition, the  $H$ -dependence of  $P$  is also consistent with earlier work. Take sample  $x=0.94$  as an example, as shown in Fig. 3(b), significant response of  $P$  against  $H$  is confirmed.

In order to understand the abnormal  $P(x)$  around  $x=1.0$ , one looks into the corresponding magnetic behaviors. Figure

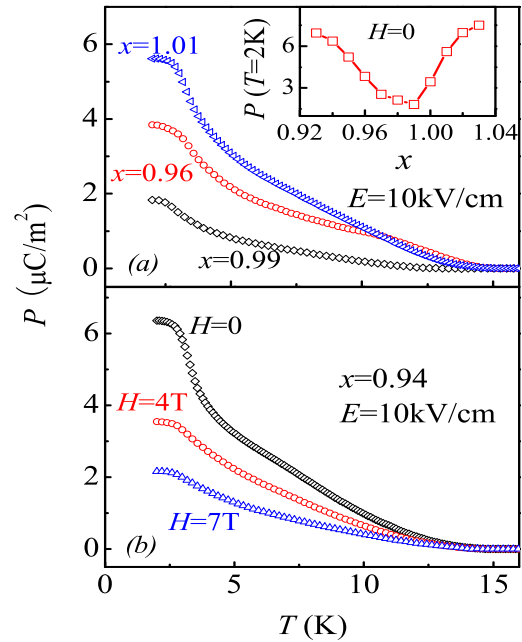


FIG. 3. (Color online) (a) Measured  $P$  as a function of  $T$ . The inset reveals measured  $P(x)$  data at  $T\sim 2$  K. (b) Measured  $P(T)$  data for  $x=0.94$  under different  $H$ .

4 shows the measured  $\chi(T)$  and  $\epsilon(T)/\epsilon(T=20$  K) for several samples.  $\chi(T)$  was measured under zero field cooling condition with a measuring magnetic field  $H=100$  Oe. It exhibits a broad peak at  $T=T_{\text{max}}$ , which is associated with the appearance of the spin LRO,<sup>3-6</sup> and  $T_{\text{max}}(x)$  is given in the inset of Fig. 4(a). Again,  $T_{\text{max}}(x)$  shows a V-shaped pattern with the lowest point at  $x\sim 0.99$ , in accordance with earlier report.<sup>4</sup> The one-to-one correspondence between  $T_{\text{max}}$  and the disappearance point of  $P$  indicates the multiferroic behavior in terms of the coupling between the FE and spin orders.

For  $\epsilon(T)$ , although similar behavior applies to all the samples, the relative dielectric fluctuations around the tran-

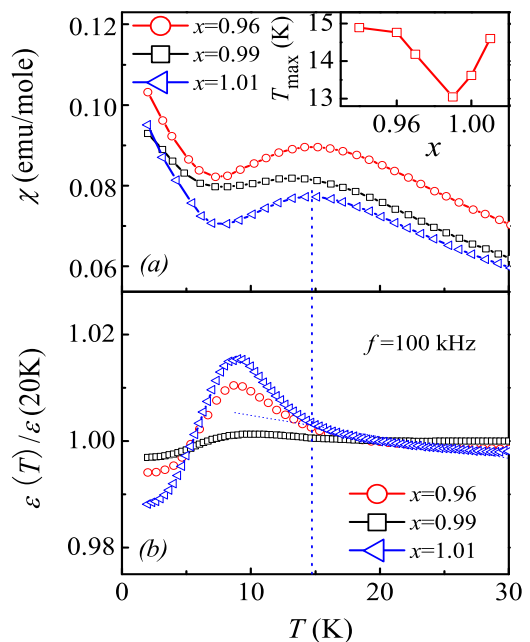


FIG. 4. (Color online) (a) Measured  $\chi$  as a function of  $T$  under  $H=100$  Oe, with the inset showing  $T_{\text{max}}(x)$ . (b) Measured  $\epsilon(T)/\epsilon(T=20$  K). Dashed line shows the high- $T$  linear behavior of  $\epsilon$  for sample  $x=1.01$ .

sition point for the FE and spin orders are very different. While no much dielectric fluctuations for  $x=0.99$  are identified, suggesting the small  $P$ , the fluctuations for  $x=0.96$  and  $1.01$  are much more remarkable. The dashed line in Fig. 4(b) labels the temperature for sample  $x=1.01$  at which the dielectric anomaly begins to appear and the magnetic order develops.

Given the presented data on the FE, dielectric, and magnetic properties of CCMO for various Co:Mn ratios, one may have basis to look into the microscopic mechanism for the dependence of multiferroicity on the Co:Mn ratio. We first consider the impact of the Co:Mn ratio on the spin order. For one-dimensional Ising chains, the spin LRO could not maintain if only the intrachain NN ferromagnetic interactions ( $J_F$ ) and NNN antiferromagnetic (AFM) interactions ( $J_{AF}$ ) [Fig. 1(b)] are considered,<sup>4,14,15</sup> suggesting the interchain spin interactions must be the ingredient for stabilizing the spin LRO. As shown in Fig. 1(b) from Ref. 4, the most favorable interchain superexchange path is the NNN Co-Co AFM interaction  $J'$ . This path forms an infinite spiral along the three adjacent chains and is thus geometrically frustrated. As a result, the interchain spin structure is probably set by another interaction path  $J''$ , which forms a spiral with a shorter pitch and lacks frustration. However, the long-range effective coupling ( $J_4$ ), which arises from  $J'$ , tends to destabilize this spin structure and the competition between  $J_4$  and  $J''$  thus gives rise to the incommensurate state and suppresses the spin LRO at  $x \sim 1$ .<sup>4,16</sup> This means that the existence of  $J_4$  damages the FE polarization. However, it is also suggested that  $J_4$  can be affected significantly by the Co/Mn ionic disorder, which may be sufficient to disrupt this interaction.<sup>4</sup> In this case, a degree of ionic disorder to certain extent would help to suppress  $J_4$  and surprisingly lead to the appearance of commensurate state and the LRO, since the competition between  $J_4$  and  $J''$  is suppressed. Given the scenario above, a strict stoichiometry of  $x=1$  does not benefit to the stability of the spin LRO, while instead a slight ionic disorder by deviating the Co:Mn ratio from one does. The magnetic data in Fig. 4 do support this scenario: in the inset,  $T_{\max}(x)$  takes a V-shape, suggesting the V-shaped stability of the LRO as a function of  $x$ .

Based on this scenario, it is easy to understand the V-shaped  $P(x)$  relation revealed in our experiment. We illustrate the underlying mechanism in Fig. 1. In Figs. 1(c)–1(f), the white (open) bars represent the FE domains with upward  $P$  along which the poling electric field  $E$  is applied, while the red (black) bars represent those with downward  $P$ . The two types of domains are degenerate in energy. For sample  $x=1.0$ , the spin LRO is greatly suppressed by the competing interactions and thus the FE domains are relatively small in size. Under the poling field, all the FE domains are aligned along the  $E$  direction at low  $T$ , e.g., 2 K, as shown in Fig. 1(c). Upon removal of the poling field, these small domains are easily flipped, activated by thermal fluctuations, leading to the coexistence of the two types of FE domains with almost identical volume fractions, as shown in Fig. 1(d). Thus, the eventually measured net polarization is very small due to the  $P$  cancel of these opposite domains.

When the Co:Mn ratio deviates from one ( $x$  deviates from 1.0), the local Co/Mn ionic disorder allows enhancement of the bulk spin LRO and thus the formation of large FE domains, as shown in Figs. 1(e) and 1(f). Again, under

the poling field  $E$ , the sample is cooled down to low  $T$ , e.g., 2 K, at which all the FE domains align upward, see Fig. 1(e). Upon removal of the poling field, those large FE domains have relatively higher stability than the small ones against the flipping driven by the thermal fluctuations at  $T=2$  K. Eventually, the as-formed domain pattern is shown in Fig. 1(f), which does offer a net polarization larger than the sample  $x=1.0$ .

Applying this scenario to all the samples with different Co:Mn ratios, one is in a good position to predict the V-shaped  $P(x)$  relationship, as revealed in Fig. 3(a) and the inset. Surely, it should be mentioned that further extension of the Co:Mn ratio toward a value far from  $x=1.0$  would eventually destroy the well defined ionic and spin orders shown in Fig. 1(a), thus leading to disappearance of ferroelectricity—take  $\text{Ca}_3\text{Co}_2\text{O}_6$  ( $x=0$ ) for example, which is of no ferroelectricity at all.<sup>17,18</sup>

We also need to mention that valleys of the  $P(x)$  at  $T=2$  K and  $T_{\max}(x)$  are not exactly located at  $x=1.0$  but at  $x=0.99$ . The reason may be related to the experimental uncertainty in terms of the Co:Mn stoichiometry. The complicated spin interactions and possible nonequilibrium ionic disorders arising from the sintering,<sup>1,2</sup> which is evitable even if weak, may be responsible for such an inconsistency.

This work was supported by the NSF of China (Grant Nos. 10864075 and 50832002), the 973 Plans of China (Grant Nos. 2006CB921802 and 2009CB623303), the NSF of Jiangsu Province (Grant No. BK2008024), the NSF of Guangdong Province (Grant No. 8151063101000001), and the Guangzhou City (Grant No. 2009J1-C471), China.

<sup>1</sup>S.-W. Cheong and M. Mostovoy, *Nature Mater.* **6**, 13 (2007).

<sup>2</sup>K. F. Wang, J.-M. Liu, and Z. F. Ren, *Adv. Phys.* **58**, 321 (2009).

<sup>3</sup>Y. J. Choi, H. T. Yi, S. Lee, Q. Huang, V. Kiryukhin, and S.-W. Cheong, *Phys. Rev. Lett.* **100**, 047601 (2008).

<sup>4</sup>V. Kiryukhin, S. S. Lee, W. Ratcliff II, Q. Huang, H. T. Yi, Y. J. Choi, and S.-W. Cheong, *Phys. Rev. Lett.* **102**, 187202 (2009).

<sup>5</sup>Y. J. Jo, S. S. Lee, E. S. Choi, H. T. Yi, W. Ratcliff II, Y. J. Choi, V. Kiryukhin, S.-W. Cheong, and L. Balicas, *Phys. Rev. B* **79**, 012407 (2009).

<sup>6</sup>R. Flint, H.-T. Yi, P. Chandra, S.-W. Cheong, and V. Kiryukhin, *Phys. Rev. B* **81**, 092402 (2010).

<sup>7</sup>Y. J. Guo, S. Dong, K. F. Wang, and J.-M. Liu, *Phys. Rev. B* **79**, 245107 (2009).

<sup>8</sup>H. Wu, T. Burnus, Z. Hu, C. Martin, A. Maignan, J. C. Cezar, A. Tanaka, N. B. Brookes, D. I. Khomskii, and L. H. Tjeng, *Phys. Rev. Lett.* **102**, 026404 (2009).

<sup>9</sup>X. Y. Yao, V. C. Lo, and J.-M. Liu, *J. Appl. Phys.* **105**, 033907 (2009); X. Y. Yao, V. C. Lo, and J.-M. Liu, *J. Appl. Phys.* **106**, 013903 (2009).

<sup>10</sup>Y. Zhang, H. J. Xiang, and M.-H. Whangbo, *Phys. Rev. B* **79**, 054432 (2009).

<sup>11</sup>L. Li, W. Z. Luo, Y. J. Guo, S. Z. Li, S. J. Luo, K. F. Wang, and J.-M. Liu, *Appl. Phys. Lett.* **96**, 022516 (2010).

<sup>12</sup>V. G. Zubkov, G. V. Bazuev, A. P. Tyutyunnik, and I. F. Berger, *J. Solid State Chem.* **160**, 293 (2001); S. Rayaprol, K. Sengupta, and E. V. Sam-pathkumaran, *Solid State Commun.* **128**, 79 (2003).

<sup>13</sup>S. Z. Li, C. Zhu, Z. B. Yan, S. J. Luo, K. F. Wang, and J.-M. Liu, *J. Phys.: Condens. Matter* **22**, 206005 (2010).

<sup>14</sup>P. Bak, *Rep. Prog. Phys.* **61**, 3962 (1987).

<sup>15</sup>J.-J. Kim, S. Mori, and I. Harada, *J. Phys. Soc. Jpn.* **65**, 2624 (1996).

<sup>16</sup>S. Agrestini, L. C. Chapon, A. Daoud-Aladine, J. Schefer, A. Gukasov, C. Mazzoli, M. R. Lees, and O. A. Petrenko, *Phys. Rev. Lett.* **101**, 097207 (2008).

<sup>17</sup>P. L. Li, X. Y. Yao, F. Gao, C. Zhao, K. B. Yin, Y. Y. Weng, and J.-M. Liu, *Appl. Phys. Lett.* **91**, 042505 (2007).

<sup>18</sup>X. Y. Yao, S. Dong, and J.-M. Liu, *Phys. Rev. B* **73**, 212415 (2006); X. Y. Yao, S. Dong, K. Xia, P. L. Li, and J.-M. Liu, *ibid.* **76**, 024435 (2007).